Two-dimensional electron-scattering processes on Na-dosed Cu(111): A two-photon photoemission study

X. Y. Wang, R. Paiella, and R. M. Osgood, Jr.
Columbia Radiation Laboratory, Columbia University, New York, New York 10027
(Received 18 January 1995)

Angle-resolved two-photon photoemission was used to investigate scattering of image-state electrons on Cu(111) at very low coverages of adsorbed Na atoms. The observed adsorption-induced broadening and quenching of the image-state peak are attributed to weakened conservation of the parallel momentum as well as interband, inelastic electron scattering. A phenomenological adsorbate scattering cross section, which is proportional to the parallel momentum, is introduced to characterize the nonlifetime linewidth broadening.

I. INTRODUCTION

Two-dimensional (2D) electron systems, including those at single-crystal conducting surfaces[1] as well as at numerous interfaces of interest in semiconductor devices,[2] have been the subject of considerable interest for the last few decades. In recent years, the system of alkali-metal adsorption on a single-crystal metal surface has attracted much attention[3] because of the relative simplicity of its physical phenomena and ease in sample preparation; understanding this simple system can hopefully guide our investigation of more complex solid interfaces. An interesting and analytically tractable excited-state 2D electronic system is that of the image-potential states[4] on highly polarizable surfaces. These are the bound states for an electron confined between the projected band gap of a crystal and the potential of the image charge at the surface. These states form a Rydberg series with binding energies E_n of typically $\lesssim 0.85$ eV below the vacuum level because of the Coulombic nature of the image barrier.[5] While there have been several studies of image states on alkali-adsorbed metal surfaces, where alkali-induced surface states as well as image states were observed at monolayer alkali coverages,[6] the scattering mechanisms of image-state electrons in such a system have not been extensively investigated.

In this work, we present studies of the dynamics of the 2D image-state electron on a single-crystal substrate in the presence of very low coverages ($< \frac{1}{100}$ ML) of alkali-metal adatoms. In particular, we have performed an angle-resolved, two-photon photoemission (2PPE) investigation of the scattering of the $n=1$ image-state electrons by nearly ionized surface species introduced through the adsorption of Na on Cu(111). The 2PPE technique has proven[5] to be a useful method for observing these normally unoccupied image states because of its high-energy resolution. The use of angle-resolved photoemission allows us to study selectively the dynamics of electrons with a given, unique lateral velocity, unlike, for instance, transport-measurement techniques in which the appropriate parameters are averaged over a few kT about the Fermi energy.[7] The interaction of a 2D Fermi gas with Coulombic scattering centers has been previously studied in relation to semiconductor interfaces,[8] where it represents one of the main factors limiting electron mobility. By using the angle-resolved 2PPE technique, we can distinguish and characterize two different scattering mechanisms, i.e., the inelastic scattering, where image-state electrons are scattered into bulk states, and the elastic scattering, where nonlifetime features are encountered.

II. EXPERIMENT

In the experiment we chose to examine the $n=1$ image stage on Cu(111). The image state on this surface can be efficiently excited from the well-known Gartland-Slagsvold (GS) surface state[9] located ~ 0.4 eV below the Fermi level. In addition, because this image state lies near the top of the projected *s-p* hybridization gap at $k_{\parallel} \sim 0$, the density of available unoccupied bulk states, which can serve as Auger decay channels for the image state, is low in its vicinity. Thus a strong photoemission signal can be obtained using resonant 2PPE, with the GS state as the initial state, at relatively moderate UV intensities, permitting us to study the behavior of the image state over a relatively wide range of alkali-metal coverage. The Cu(111) sample (99.999% purity) was mechanically and chemically[10] polished before being loaded in the UHV chamber, and then subjected to multiple-sputter (2 kV, 5×10^{-5} Torr of argon)-anneal ($\lesssim 800$ K) cycles until a sharp low-energy electron-diffraction (LEED) pattern was observed. The scattering centers were introduced by depositing controlled amounts of Na onto the sample from a well-outgassed commercial getter source (SAES, Inc.). The chamber base pressure was typically $\sim 6.5\times10^{-11}$ Torr during the measurements, and always $< 1.0\times10^{-10}$ Torr during Na evaporation. The experiments were performed with 20-ns, *p*-polarized laser pulses generated from a three-stage excimer-laser-pumped tunable dye laser. The frequency-doubled laser pulses of photon energy $h\nu = 4.47$ eV, which is roughly equal to the energy of the resonant transition between the intrinsic surface state and the $n=1$ image state,[11] were used to

excite the image state on Cu(111). The intensity of the incident light was kept low enough to avoid sample heating and space-charge effects. The electron-energy-distribution curve (EDC) was analyzed with an electrostatic, 160° spherical-sector analyzer coupled to a pair of microchannel plates and a transient digitizer. The acceptance cone of the detector is about 0.002 sr, giving a momentum resolution of ~ 0.05 Å^{-1} for the measurements presented here. The detector energy resolution could be set as high as 60 meV. However, in practice, the detector resolution was set at ~ 95 meV in order to obtain a good signal-to-noise ratio throughout the experimental range. In the angle-resolved experiment, the incidence angle of the laser pulse was fixed at 68° while the detector was rotated with respect to the sample surface in the incidence plane; the accuracy of this rotation was better than ±0.2°. The sample was biased −4.0 V in order to help eliminate the effects of any possible stray magnetic field and space charge.

III. RESULTS AND DISCUSSION

A typical photoemission EDC from a clean Cu(111) surface at normal emission is shown in Fig. 1. The peak at the low energy is due to electrons photoexcited from the thermal tail of the Fermi distribution by one-photon photoemission (1PPE). The peak at ~ 3.65 eV above the vacuum level, $E_{\rm vac}$, is due to 2PPE from the $n=1$ image state. The binding energy (relative to $E_{\rm vac}$), $E_B = 0.82 \pm 0.02$ eV, is calculated from $(h\nu - E_{\rm kin})$, where $E_{\rm kin}$ is the electron kinetic energy above the vacuum level. Our measured value agrees well with the values given in Refs. 11 and 12. The intrinsic linewidth of the 2PPE peak was determined by fitting the peak with a convolution of the Lorentzian line shape for the image state and a Gaussian response function of the electron energy analyzer.[13] The Gaussian detector linewidth $\Gamma_{\rm res}$ was set to 95 meV (FWHM), a value which was determined by a measurement of the low-energy cutoff of the 1PPE peak.[13,14] The nonlinear least-square fit of the experimental data and the deconvolution yielded an intrinsic FWHM of $\Gamma = 25 \pm 10$ meV for the $n=1$ image state on Cu(111), in fair agreement with the value $\Gamma = 16 \pm 4$ meV from previously reported.[13] This approach was verified through a separate technique which measured the $n=1$ peak width at different values of detector energy resolution and then extrapolated the linewidth to zero resolution, giving the result of $\Gamma = 20 \pm 8$ meV. Interestingly, the width of the $n=1$ feature was found to be sensitive to the quality of surface preparation.

The evolution of the image-potential peak at normal emission under conditions of the same excitation intensity on the Cu(111) surface at Na coverages, fro $m\Theta = 0$ to $\Theta = \frac{9}{1000}$ ML, is shown in Fig. 2. The Na deposition on Cu(111) was monitored by the alkali-induced change in work function. At low coverages the adsorbed atoms are highly polarized[3] normal to the surface, forming electric dipoles that dramatically decrease the dipolar portion of the bare-surface work function. The work-function change is measured from the shift in the low-energy cutoff of the 1PPE peak. The amount of Na coverage is then calibrated against a previously reported[15] work-function-vs-coverage curve for Na on Cu(111). These results can be verified independently by separate coverage-dependent LEED measurements. Specifically, we observed the characteristic disordered overlayer structure throughout the low coverage range ($\lesssim \frac{1}{100}$ ML), followed by the gradual development of a ringlike diffraction pattern at higher coverage, until finally an ordered $(\frac{3}{2} \times \frac{3}{2})$ hexagonal Na adsorption structure appeared at a coverage of about 0.4 ML, consistent with results described in Ref. 15.

Figure 2 shows a sharp decrease in the photoemission

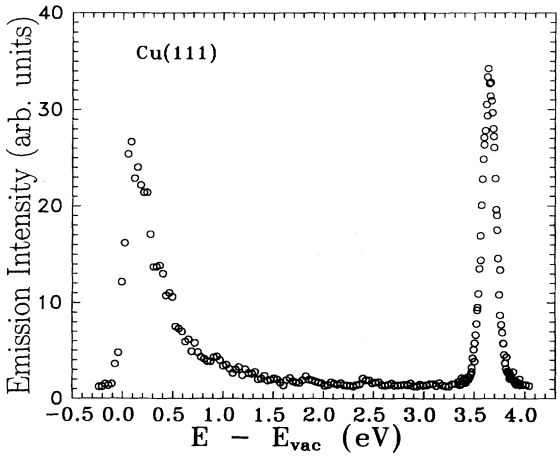

FIG. 1. A typical photoemission energy-distribution curve (EDC) obtained at normal emission from Cu(111), excited by laser pulses of 4.47-eV photon energy. The low-energy peak originates from the Fermi tail through a 1PPE process, and the sharp peak at higher energy is due to 2PPE with the $n=1$ image state as the intermediate state.

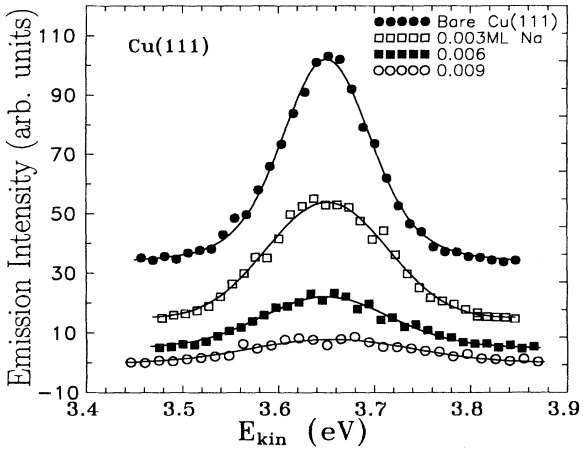

FIG. 2. EDC's from the $n=1$ image state at normal emission from Cu(111) in the presence of a Na adsorbate, at coverages of $\Theta = 0$, $\frac{3}{1000}$, $\frac{6}{1000}$, and $\frac{9}{1000}$ ML, respectively. The fit to the data was obtained by a convolution of a Gaussian and a Lorentzian line shape as described in the text, using a nonlinear least-square algorithm.

intensity upon Na adsorption; in fact, at a coverage as low as 0.012 ML, the image state appeared to be completely quenched. In addition, the image peak was significantly broadened with Na coverage. Also note that the energetic position of the peak does not appear to shift with coverage, even though the work function, as measured from the low-energy cutoff of the 1PPE peak, does decrease significantly with Na coverage, e.g., ~ 0.35 eV at a coverage of 0.009 ML. This result suggests that the observed image state exists only in bare regions of the surface where the effect of the Na-adsorption-induced dipoles on the work function is minimal. In these regions, the local work function[16] is the same as on the clean surface; in contrast, the experimentally measured work function is a value averaged over a macroscopic area of the inhomogeneously covered surface. Since image states are energetically pinned to the vacuum level,[17] photoelectrons from the image state are thus detected at the same kinetic energy as from the bare surface.

In order to characterize the quenching and linewidth broadening mechanisms shown in Fig. 2, we performed an angle-resolved 2PPE study. First, the dispersion curve for the image-state band was measured since information on the effective mass of the $n=1$ image state is needed for the linewidth analysis. The angle-resolved detection system, at a fixed bias, was first calibrated against the well-known dispersion relation for the $n=1$ image state on Cu(100).[18] For bare Cu(111), the fitting of the free-electron-like parabolic $E_{\rm kin}-k_{\parallel}$ curve gives an effective mass $m^*=(1.0\pm0.1)m_e$, which is in good agreement with other observations,[12] and where $E_{\rm kin}$ is the detected kinetic energy and $k_{\parallel}$ is the parallel component of the wave vector of the emitted electrons. For the case of Na-adsorbed Cu(111) surfaces, the measurements yield values of effective masses that are nearly the same as that of the bare surface, except for an apparent $\sim 20\%$ decrease seen in m^* at $\Theta\sim\frac{1}{100}$ ML. In order to simplify the analysis described below, we have taken $m^*=m_e$ throughout the range of Θ investigated. However, we do note in passing that a similar reduction in effective mass has been seen for image-state electrons upon adsorption of a monolayer of xenon or heavy organics on Ag(111); in these cases the effect was attributed to the screening of the interaction of the image-state electrons with the bulk states by the adlayer.[19] Further investigation of the apparent reduction seen at $\Theta\sim\frac{1}{100}$ ML is planned.

The broadening of the image-state linewidth as a function of electron momentum parallel to the Cu(111) surface is shown in Fig. 3 for the clean surface and for different Na coverages. The parallel component of the emitted electron's wave vector $k_{\parallel}$ is given by $[2m_eE_{\rm kin}/\hbar^2]^{1/2}\sin\theta$, where θ is the detection angle relative to the surface normal. The Lorentzian natural linewidths shown were derived based on numerical deconvolution of the measured peak widths using the known detector Gaussian line shape, as described earlier. The linewidth is clearly seen to increase with $k_{\parallel}$ as well as Na coverage Θ in all cases. At a given coverage, the relation between the linewidth Γ and $k_{\parallel}$ appears to be parabolic. With higher Θ, the parabolic curvature becomes steeper. The basic trend of linewidth broadening as a function of $k_{\parallel}$ is similar to prior observations in the intrinsic linewidth broadening of the GS surface state,[20,21] both for the case of unintentional surface imperfections and for dosed K-adsorbate atoms.

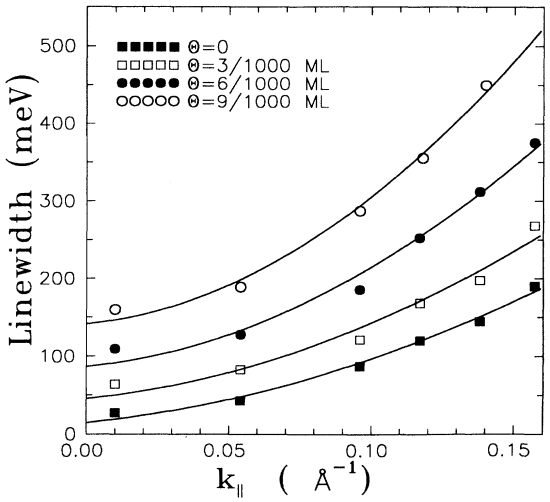

FIG. 3. The image-stage ($n=1$) linewidth broadening as a function of the electron momentum parallel to the surface, $k_{\parallel}$, on clean and Na-adsorbed Cu(111), at coverages of $\Theta=\frac{3}{1000}$, $\frac{6}{1000}$, and $\frac{9}{1000}$ ML, respectively.

The contributions to the measured linewidth can be analyzed as follows. First, since 2PPE involves three levels—initial, intermediate, and final—the measured linewidth for the process can in principle involve contributions from all three states. However, recent measurements[13] for the case of Cu(111) have shown conclusively that this process is incoherent; that is, the two steps are dephased with respect to each other. For this case, the measured linewidth is independent of the initial state. Further, because the intermediate image state is a surface state, which lacks dispersion in the direction normal to the surface, the contribution from the final state is absent.[22] As a result, the linewidths measured here are readily interpreted as those solely of the image state, without complications from the initial and final states.

Broadening of the image-state linewidth can be attributed to both lifetime and nonlifetime effects. The lifetime-related linewidth involves the decay of image-state electrons into empty bulk states, as well as inelastic scattering from defects, intrinsic impurities, and intentionally introduced Na scattering centers, whether neutral or ionic. This reduction in lifetime has a direct impact on the image peak intensity, since the image-state electron signal is directly proportional to the average number of electrons in the image state during the laser-excitation pulse. Clearly, the signal intensity from the 2PPE process is also directly related to the population of the initial surface state, which on the bare surface is fully occupied due to its location well below the Fermi level. However, an earlier experiment[21] using one-photon photoemission showed that the adsorption of alkali metal has little effect on the occupancy of this surface state at low

alkali coverages such as used here, e.g., $<\frac{1}{100}$ ML. Therefore, any change in the 2PPE signal intensity (integrated) for the measurements presented here can be attributed solely to lifetime changes associated with the image state. Thus, for example, a factor of 2 increase in lifetime broadening would then imply a factor of 2 reduction in the measured total signal. In the case of nonlifetime broadening, which is a result of the elastic-scattering process, the number of electrons in the image state or the total signal from the 2PPE EDC would not vary with changes in broadening. Therefore, it is possible, in principle, to make an assessment and separation of the contributions from the lifetime and nonlifetime mechanisms by analyzing the reduction in signal intensity in connection with the corresponding linewidth broadening. By numerically integrating the area under the EDC's shown in Fig. 2, the relative image-state signal was found to be $S_1:S_2:S_3:S_4=4.1:3.0:1.5:1.0$ for Na coverages of 0, $\frac{3}{1000}$, $\frac{6}{1000}$, and $\frac{9}{1000}$ ML. respectively, obtained under the *same* excitation conditions (including the laser incidence angle and intensity on the sample). The corresponding linewidth broadening is $\Gamma_1:\Gamma_2:\Gamma_3:\Gamma_4=1.0:3.1:5.6:8.4$ (see Fig. 3 at $k_{\parallel}\sim 0$). Since any reduction in the total emission signal depends solely on the shortening of the lifetime, the contribution from inelastic scattering is approximately equal to the nonlifetime contribution; each contributes $\sim 50\%$ to the total broadening for the image state at $k_{\parallel}=0$.

The nonlifetime broadening comes from weakened conservation of momentum $\hbar k_{\parallel}$ caused by elastic-scattering processes and mediated by surface defects or, alternately, impurities. This scattering results in electron confinement, thus mixing states of different lateral momenta. As a result, photoelectrons from each scattered image-potential state are emitted over a range of parallel wave vectors, $k_{\parallel}$, so that a 2PPE peak detected along any given angle is comprised of electrons over a range in energy, resulting in a nonlifetime broadening of the linewidth. Nonlifetime broadening of a surface state has been observed and analyzed by Kevan and Tersoff[20] in relation to angle-resolved photoemission from the GS surface state on Cu(111), where the linewidth of this state would diminish as the surface band disperses upward toward E_f—if $k_{\parallel}$ was truly conserved. In fact, they observed an increase in linewidth broadening as $k_{\parallel}$ increased, similar to the observations shown in Fig. 3 for the case of image states. In their treatment,[20] the finite width in the momentum space, $\Delta k_{\parallel}^{s}$, of the elastically scattered states can be taken to be equal to the inverse mean free path for intraband scattering.

$$\Delta k_{\parallel}^{s}=\sigma\Theta/\Omega \ , \tag{1}$$

where σ is the scattering cross section for these processes, Θ/Ω is the surface density of scattering centers, Ω the area of the substrate surface unit mesh, and Θ the coverage in monolayers. This expression implicitly assumes that scattering isotropic.

Finally, the measured linewidth must also include the effect of detector momentum resolution $\Delta k_{\parallel}^{\rm res}$, in addition to the consideration of its energy resolution. The total momentum broadening to the linewidth can be written in the notation of Ref. 20 as

$$\begin{aligned}\Gamma(\Delta k_{\parallel})&=E(k_{\parallel}+\Delta k_{\parallel}/2)-E(k_{\parallel}-\Delta k_{\parallel}/2)\\&=\hbar^2 k_{\parallel}\Delta k_{\parallel}/m^* \ ,\end{aligned} \tag{2}$$

where $\Delta k_{\parallel}=\Delta k_{\parallel}^{\rm res}$. Rigorously speaking, Eq. (2) is valid only when $k_{\parallel}>\Delta k_{\parallel}/2$. For $k_{\parallel}\sim 0$, the electron lateral kinetic energy at the detector is nonzero because of the finite $\Delta k_{\parallel}$ and the measured linewidth at $k_{\parallel}\sim 0$ is then given by $\hbar^2(\Delta k_{\parallel})^2/2m^*$. When all contributing factors mentioned above are combined, an expression for the measured linewidths, as shown in Fig. 3, is obtained for $k_{\parallel}>\Delta k_{\parallel}/2$,

$$\begin{aligned}\Gamma&=\Gamma_{\rm lifetime}+\Gamma(\Delta k_{\parallel})\\&=\Gamma_{\rm lifetime}+\hbar^2 k_{\parallel}(\Delta k_{\parallel}^{s}+\Delta k_{\parallel}^{\rm res})/m^* \ ,\end{aligned} \tag{3}$$

where $\Gamma_{\rm lifetime}$ is the contribution from inelastic-scattering events and is lifetime related, and where Lorentzian widths are assumed for both $\Gamma_{\rm lifetime}$ and $\Gamma(\Delta k_{\parallel})$. In this expression the second term (nonlifetime related) clearly exhibits both $k_{\parallel}$ and Θ dependence. In general, the possibility that $\Gamma_{\rm lifetime}$ is also dependent on $k_{\parallel}$ as well as Θ should be considered. Indeed, our angle-resolved data on *bare* Cu(111) show that the *integrated image-state signal* does decrease parabolically with increasing $k_{\parallel}$, indicating that $\Gamma_{\rm lifetime}$ is in fact $k_{\parallel}$ dependent. This lifetime broadening, as determined from the signal reduction in the EDC data as a function of $k_{\parallel}$, contributes about $\frac{1}{3}$ of the total broadening shown in Fig. 3 for $\Theta=0$. However, in the case of Na-adsorbed Cu(111), a similar analysis shows only an insignificant lifetime broadening as a function of $k_{\parallel}$, and hence $\Gamma_{\rm lifetime}$ can be regarded as $k_{\parallel}$ independent in the following analysis.

Using Eq. (3), we numerically fit the linewidth-vs-$k_{\parallel}$ data shown in Fig. 3, using the experimental detector momentum resolution of $\Delta k_{\parallel}^{\rm res}=0.05$ Å^{-1}. The least-square fitting shows $k_{\parallel}^2$-dependent broadening at the four Na coverages of Fig. 3. Elastic scattering occurs both through the controlled surface-Na species, as expressed in Eq. (1), and through intrinsic impurity and defects unrelated to Na adsorption, denoted by the factor $\Delta k_{\parallel}^{0}$. Therefore, one can write

$$\Delta k_{\parallel}^{s}=\Delta k_{\parallel}^{0}+\Theta\sigma/\Omega \ , \tag{4}$$

where $\Delta k_{\parallel}^{0}$ is given by the broadening at $\Theta=0$, i.e., $k_{\parallel}\Delta k_{\parallel}^{0}=0.4k_{\parallel}^{2}$. Equation (4) can be used to obtain a Na-induced scattering cross section $\sigma=(83\pm 16)\Omega k_{\parallel}$, valid for all three Na coverages. This empirical expression indicates a direct proportionality with the parallel momentum for the scattering cross section of image-state electrons. This result does not appear to be in accord with conventional Coulombic scattering theory, which would suggest that the scattering cross section should be inversely proportional to $k_{\parallel}$.[23] However, the elastic-scattering process involved here results in the mixing of quantum states, rather than a simple Coulombic-type scattering event, thus deviation from a Coulombic scattering cross section may be anticipated. Note that

for $k_{\parallel}=0.1$ Å^{-1} and $\Omega=5.7$ Å^2 for the Cu(111) surface,[24] we find $\sigma=47\pm9$ Å, which is about an order of magnitude larger than the value found for the broadening of one-photon EDC's from the GS surface state on *K*-covered Cu(111), using angle-resolved photoemission.[21]

Other experiments have measured linewidth broadening effects only at normal emission. For comparison in our experiments, at $k_{\parallel}\sim0$, a nearly linear relation is found between image-state linewidth and coverage with a slope of about 12 eV/ML. This value is significant larger than that reported from the O/Ni(100) system, with a coverage-dependent broadening of 1.2 eV/ML.[13] Recent studies of image states in the Ag/Cu(111) adsorption system[25] offer an interesting contrasting system. In such a noble-metal adsorbate system, the Cu(111) $n=1$ image state does not exhibit significant quenching and broadening until $\gtrsim0.6$-ML coverage, at which point the *Ag-induced* $n=1$ and 2 image states become prominent and remain so until they dominate for $\Theta\gtrsim1$ ML. The lack of strong broadening effects in this case is in contract to the fact that alkali-metal adsorbates give rise to particularly strong induced-dipole moments; such a polarized adsorbate would be expected to be a particularly efficient scattering center for lateral confinement and inelastic lifetime quenching.

Finally, preliminary studies have been performed on the $n=2$ image state at photon energies close to the energy difference between the GS surface state and the $n=2$ state. The experiment shows quenching and broadening of nearly the same magnitude as for the $n=1$ state. This is not an unexpected result, since an image-state electron in either the $n=1$ or 2 state is approximately an equal average distance from a Na-induced dipole, for the low coverages used here. In particular, for the maximum coverage used, i.e., ~0.01 ML, the average interatomic spacing for the Na adatoms is ~30 Å, a value much larger than the average distance from the surface for $n=1$ and 2 of ~2 and ~10 Å, respectively.[26]

IV. CONCLUSION

In summary, we have performed angle-resolved 2PPE measurements of image-state electron scattering on a Cu(111) surface adsorbed with Na atoms. The measurements show drastic quenching and broadening effects on the image state at very low Na dosage ($<\frac{1}{100}$ ML) in comparison with other adsorption systems. The nonlifetime linewidth broadening shows significant lateral confinement of the image-state electrons by the introduced Na scattering centers through elastic collisions. An empirical scattering cross section is obtained and found to be proportional to the parallel momentum of the image-state electron. This 2PPE momentum-resolved technique can be widely applicable to other simple interface systems in studying 2D excited-state electron-scattering mechanisms.

ACKNOWLEDGMENTS

We gratefully acknowledge the financial support of this work by the Columbia JSEP Program (Contract No. DAAH04-94-G-0057) and the Army Research Office (Contract No. DAAL03-92-G-0191). In addition, we thank K. C. Chau for assisting in programming the data-processing instrumentation. Finally, we are grateful to Dr. J. Tersoff for several stimulating and helpful discussions.

[1]E. G. McRae, Rev. Mod. Phys. **51**, 541 (1979); F. J. Himpsel, Adv. Phys. **32**, 1 (1983).

[2]E. H. Rhoderick and R. H. Williams, *Metal-Semiconductor Contacts* (Oxford Science Publications, Oxford, 1988); J. Singh, *Physics of Semiconductors and Their Heterostructures* (McGraw-Hill, New York, 1993).

[3]H. P. Bonzel, A. M. Bradshaw, and G. Ertl, *Physics and Chemistry of Alkali Metal Adsorption* (Elsevier, Amsterdam, 1989); Prog. Surf. Sci. **42** (1993).

[4]P. M. Echenique and J. B. Pendry, J. Phys. C **11**, 2065 (1978).

[5]W. Steinmann, Appl. Phys. A **49**, 365 (1989).

[6]N. Fischer, S. Schuppler, R. Fischer, Th. Fauster, and W. Steinmann, Phys. Rev. B **47**, 4705 (1993).

[7]T. Ando, A. B. Fowler, and F. Stern, Rev. Mod. Phys. **54**, 437 (1982).

[8]F. Stern and W. E. Howard, Phys. Rev. **163**, 816 (1967).

[9]P. O. Gartland and B. J. Slagsvold, Phys. Rev. B **12**, 4047 (1975).

[10]Y. Jee, M. F. Becker, and R. M. Walser, J. Opt. Soc. Am. B **5**, 648 (1988).

[11]K. Giesen, F. Hage, F. J. Himpsel, H. J. Riess, and W. Steinmann, Phys. Rev. B **33**, 5241 (1986).

[12]G. D. Kubiak, Surf. Sci. **201**, L475 (1988).

[13]S. Schuppler, N. Fischer, Th. Fauster, and W. Steinmann, Phys. Rev. B **46**, 13 539 (1992).

[14]H. B. Nielsen, G. Brostroem, and E. Matthias, Z. Phys. B **77**, 91 (1989).

[15]X. Shi, D. Tang, D. Heskett, K. D. Tsuei, H. Ishida, and Y. Morikawa, Surf. Sci. **290**, 69 (1993).

[16]R. Fischer, S. Schuppler, N. Fischer, Th. Fauster, and W. Steinmann, Phys. Rev. Lett. **70**, 654 (1993).

[17]Z. Wu, B. Quiniou, J. Wang, and R. M. Osgood, Jr., Phys. Rev. B **45**, 9406 (1992).

[18]K. Giesen, F. Hage, F. J. Himpsel, H. J. Rieβ, and W. Steinmann, Phys. Rev. B **35**, 971 (1987).

[19]D. F. Padowitz, W. R. Merry, R. E. Jordan, and C. B. Harris, Phys. Rev. Lett. **69**, 3583 (1992); W. R. Merry, R. E. Jordan, D. F. Padowitz, and C. B. Harris, Surf. Sci. **295**, 393 (1993).

[20]S. D. Kevan, Phys. Rev. Lett. **50**, 526 (1983); J. Tersoff and S. D. Kevan, Phys. Rev. B **28**, 4267 (1983).

[21]S. D. Kevan, Phys. Rev. B **33**, 4364 (1986); Surf. Sci. **178**, 229 (1986).

[22]N. V. Smith, P. Thiry, and P. Petroff, Phys. Rev. B **47**, 15 476 (1993).

[23]See, for example, L. I. Schiff, *Quantum Mechanics* (McGraw-Hill, New York, 1968).

[24]L. J. Clarke, *Surface Crystallography* (Wiley, New York, 1985).

[25]Th. Fauster and W. Steinmann, in *Electromagnetic Waves: Recent Developments in Research,* edited by P. Halevi (Elsevier, Amsterdam, 1995), and references cited therein.

[26]D. Straub and F. J. Himpsel, Phys. Rev. B **33**, 2256 (1986).